NI

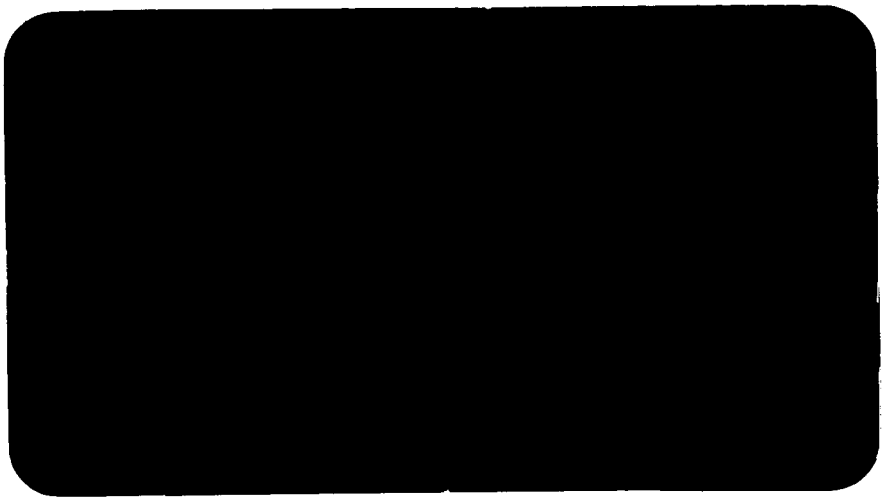

ASTRO

RESEARCH CORPORATION

SANTA BARBARA, CALIFORNIA

Copy_____of_____
Series_____

ARC-R-219

THE SPINNING FILAMENTARY DISK AS A HYPERSONIC DECELERATOR

AUGUST 25, 1966

Submitted under Contract NAS7-427

Prepared by:

RICHARD H. MACNEAL, and
ALBERT C. KYSER

Approved by:

HANS U. SCHUERCH

ASTRO RESEARCH CORPORATION
P. O. BOX 4128
SANTA BARBARA, CALIFORNIA
TEL: 963-3423

CONTENTS

ABSTRACT

By spinning a flexible disk about a central hub, it is possible to erect a surface which is sufficiently stiff to be useful for aerodynamic braking. Such a disk is potentially useful as a reentry decelerator because it can be made relatively large with reasonable weight. If the area is large enough, radiation cooling will keep the surface temperature within tolerable limits without the use of non-structural thermal-protection materials. The paper presented here describes a reentry decelerator system, called the "Rotornet", that exploits these possibilities. The disk area required for typical manned reentry missions from earth orbit is of the order of one square foot per pound of payload, and the decelerator weight is a few percent of the payload weight. The advantages of such a system are greatest under conditions of long heating pulses (e.g., manned entry at superorbital speeds) or low-density atmosphere (e.g., Mars). The Rotornet is shown to be free from spiral instability with proper mass balance and rotor coning. The rotor disk exhibits travelling-wave panel flutter which can be suppressed by various means.

I. INTRODUCTION

The possibility of using large, lightly loaded decelerators for entry from orbit into planetary atmospheres has been of continuing interest since the beginning of serious work in reentry mechanics. Eggers[1] and Gazley[2], as well as other early investigators, have pointed out that for a ballistic vehicle of given mass the maximum heating rate decreases as the effective drag area $C_D A$ is increased. Thus, if the drag area can be made sufficiently large, the heating rates can be made compatible with the ability of structural materials to reject heat by radiation.

The principal advantage to be gained from the large-drag-area approach is that for a wide range of mission parameters it offers a potentially large decrease in the decelerator weight fraction (ratio of decelerator weight to payload weight) over the use of systems of conventionally high density. In addition, there are a number of important secondary advantages, such as operation at lower temperatures, improved communication throughout

the descent, and a potential for gliding and maneuvering without large increases in structural weight.

Most of the devices which have been proposed to take advantage of this operating regime have been towed decelerators (e.g., parachutes, balloons, Ballutes, cones, paragliders).[3] These devices share a number of basic problems; for example, they must operate in the unsteady wake of the payload, and they experience excessive and uneven heating on shroud lines and points of shock impingement. As a result, the towed decelerator has not been competitive with ablative systems for the reentry problem.

There have been at least two important attempts to bypass some of the problems of the towed decelerator by mounting the drag surface on the nose of the payload. One of these, the Avco drag brake,[4] showed considerable promise but suffered from the weight penalty associated with carrying the structural loads in bending over large spans. A more recent development of this type is the tension-cone decelerator,[5,6] which makes use of a conical membrane to transmit the aerodynamic loads to the payload, and a concentrated ring to carry the compression forces

necessary to hold the membrane erect. This scheme appears very promising for missions such as the Mars Lander, and is currently under active development. Because of the weight associated with the compression ring, however, it appears likely that this device will not be feasible in sizes large enough to permit operation without considerable weight in thermal protection.

The decelerator system described here, which has been named the "Rotornet", grew out of an attempt to reduce the decelerator weight fraction by eliminating the requirement for stiff structure to hold the surface erect. In the Rotornet system, the aerodynamic surface is formed by a rapidly spinning filamentary disk. It has been found that this concept makes possible the use of aerodynamic surfaces which are sufficiently large to permit reentry deceleration without non-structural thermal protection. The purpose of this paper is to present the work which has been done on the Rotornet concept, to discuss its potential usefulness, and to point out areas in which important work remains to be done.

II. GENERAL DESCRIPTION

The aerodynamic surface which is the basic element of the Rotornet system is a large, lightweight, filamentary disk, mounted at its center to a hub on the nose of the payload, as shown in Figure 1, and maintained in a deployed condition by the centrifugal effects associated with a high spin rate. The disk is constructed with continuous fibers that run in curved paths from hub to rim and back, in an axisymmetric fiber pattern such that the tension throughout the disk is (essentially) uniform under the loading of its own inertia in the centrifugal field. The aerodynamic surface is therefore composed of a bidirectional array of structural fibers under tension.

The texture of the filamentary disk is that of a sleazy fabric with the bias direction coinciding at every point with the radial direction on the disk. The surface can therefore deform locally, through the mechanism of trellis shear, without changes in fiber length and without wrinkling. This geometry allows the spinning disk to deform into a cone without gross changes in the stress

distribution. Under the aerodynamic loading, the disk "cones back", and the load is transmitted to the hub in the form of an axial component of fiber tension. For the Rotornet systems under consideration here, the coning is limited by heating considerations (for this study) to a coning angle of about 30° (cone half-angle of 60°), since it is essential to maintain the detached shock system characteristic of blunt bodies.

Around the periphery of the disk are attached a number of small weights, with an aggregate mass equal to perhaps twenty percent of the mass of the disk. These tip weights serve to improve the behavior of the fabric disk during deployment and in operation at lower altitudes. They may (for missions requiring gliding and maneuvering) have the form of aerodynamic vanes to counteract the aerodynamic friction torque of the disk; for the ballistic reentry mission, however, the Rotornet system can operate on the energy of the initial spin-up, without sustaining torque.

The fibers of the net are attached to the hub by a clamp ring having a diameter of perhaps fifteen percent

of the disk diameter. If the payload cannot withstand the spin rate, the clamp ring must be attached to the payload through a bearing.

Since the rotational inertia of the deployed disk is very large compared to that of the payload, the energy for the initial spin-up must be provided by rocket motors. This spin-up energy may be obtained from retro-rockets by mounting them on the rim of the nose cap, canted to produce a reaction torque. Alternatively, the spin-up may be accomplished with small rocket motors mounted on the rim of the disk, which motors would be started after the disk is deployed and "stiffened" in rotation at a relatively low spin rate.

The operational sequence of the Rotornet in a ballistic reentry from orbit is shown in Figure 1. After deployment and spin-up of the disk and ejection from orbit, the vehicle loses altitude. The coning angle gradually increases to a maximum of about 30°, after which it decreases. In typical earth entries without lift capability, low supersonic speeds are reached at altitudes above 200,000 feet, thereby permitting potentially large

terminal-glide range. By providing a means to produce a controlled pitching moment, nonaxial (lifting) flight can be achieved. This possibility offers potentially large increases in performance, and should therefore be considered one of the goals of any development of this concept.

III. MECHANICS OF THE FILAMENTARY DISK

The Rotornet is basically a uniform-stress (isotensoid) disk, as described in References 7 and 8. The fiber geometry of the flat disk, shown in Figure 2, consists of a network of circular-arc fiber paths which intersect the origin. The fiber-path curvature is necessary for the uniform-stress condition, and must be maintained, as in a net, by "pinning" the fibers at the intersections. For the Rotornet, the disk is truncated slightly, near the periphery, in order to provide support for the tip weights. The total mass of the tip weights is approximately equal to the mass of the truncated outer section.

An important characteristic of the fiber geometry is that it has uniform increments of arc length between points of intersection in the fiber pattern. The disk can therefore be deformed, without changes in arc length, into a cylinder, whereby the fiber pattern becomes an array of helices (the hub expands and the rim contracts to form the two edges of the cylinder). This deformation is diagrammed in Figure 2. It should be noted that if the disk is to be fabricated using continuous fibers, without structural seams, it must be fabricated with the topology of a cylinder rather than a strip.

The properties of the isotensoid disk form a convenient set of reference properties for the Rotornet disk. The weight of an isotensoid disk is readily computed from the geometry in terms of the total cross-sectional area of the fibers radiating from the origin, and the outside radius of the disk:

$$W_{ref} = \rho_f g a_f \cdot \frac{\pi}{2} \cdot R_{ref} \qquad (1)$$

where W_{ref} is the weight of isotensoid disk, $\rho_f g$ is the weight density of fiber, a_f is the total structural cross-section area of fiber radiating from origin, and R_{ref} is the reference radius (outside radius of isotensoid disk). For the present discussion it will be assumed that the structural weight of the Rotornet is adequately represented by

$$W_R = \rho_f g a_f \cdot \frac{\pi}{2} \cdot R \tag{2}$$

where R is the effective outside radius of the Rotornet disk, including the area of tip tabs.

The fiber stress distribution in an isotensoid disk is uniform. The stress, s_{ref}, associated with a spin rate, ω, is given by

$$s_{ref} = \frac{1}{2} \cdot \rho_f g \left(\omega R_{ref} \right)^2 \tag{3}$$

This is one-half of the stress in a spinning hoop of the same material. For the Rotornet disk, the nature of the distribution of fiber stress can be changed by changing

the tip weights. The stress distributions in a typical truncated disk, for several sizes of tip weights, are shown in Figure 3. If the spinning disk is loaded and deformed by an axisymmetric distribution of normal forces (e.g., aerodynamic pressure) the tension distribution will not change appreciably, provided the deflections are small compared to the radius.

The deformed shape of the loaded net depends on the aerodynamic load distribution. The aerodynamic load distribution, however, depends on the details of the shape. The equilibrium shape of the net, for any given set of conditions, must therefore be obtained simultaneously with the aerodynamic load and the tension distribution. Reference 9 describes a method for obtaining a family of equilibrium shapes by digital computer, by the use of an iterative technique. The aerodynamic loading is taken to be that of a Newtonian pressure distribution, i.e., a loading for which the local normal-pressure coefficient is given by $C_p = 2 \cos^2 \beta$ where β is the local coning angle. The results for a typical set of design parameters are shown in Figure 4 for various values of the coning

angle at the hub. Several coned-up shapes are shown, along with the corresponding drag coefficients.

The resultant axial force exerted by the coned-up Rotornet on the hub is

$$F_b = s_b a_f \cdot \sin\beta_b \cdot \cos\gamma_b \qquad (4)$$

where γ is the angle between the meridian and the tangent to fiber, and the subscript b denotes conditions at the hub. For all cases of interest, $\cos\gamma_b \cong 1$.

The axial component of force in the coned-up net at the hub is assumed to be equal to the total aerodynamic force on the net. An equivalent assumption is that the mass of the disk is negligible compared with the mass of the payload.

IV. PERFORMANCE

For preliminary design purposes, it is essential to be able to predict the size and weight of the Rotornet required to perform a given mission in terms of the mission parameters and the properties of the structural material used in the filamentary disk. It will be shown that algebraic "performance relations" suitable for this purpose can be derived readily by combining several fundamental relations describing the Rotornet and its operation.

A. Aerodynamic Heating.

The temperature of the Rotornet structure is computed under the assumption that the surface is heated by convection on the front sides and that this heat is rejected by radiation from both sides of the disk. The thermal capacity of the disk is neglected and the disk is assumed to be nonporous. It is further assumed that radiative heating from the shock layer is negligible compared with the convective heating. The condition for thermal equilibrium is that

$$\dot{q}_{conv} = \sigma\varepsilon(VF)T^4 \qquad (5)$$

where $\dot{q}_{conv}$ is the convective heating rate, ε is the emissivity of the surface, (VF) is the view factor, and T is the absolute temperature. The product $\varepsilon(VF)$ is given the value 1.4, to account for the fact that, while the heating takes place only on the front face of the disk, both front and rear faces reject heat by radiation, the rear face at a somewhat lower temperature.

The convective heating rate was computed by the methods of Lester Lees[10,11] and the Handbook of Astronautical Engineering.[12] The heating-rate distribution for a flat disk is given by Stainback,[12] who shows that the maximum heating rate occurs at the rim, and is about 0.82 of the stagnation-point heating of a sphere of the same radius. The heating distribution over a shallow cone was assumed to be such that the maximum heating rate occurs at the rim and has the same value as that measured for the disk. This assumption, taken together with Lees' formula for heating at the stagnation point of a sphere, gives the relation which was used for the critical heating rate of the

coned-back Rotornet:

$$\dot{q}_{conv} = K(\rho/R)^{\frac{1}{2}} \cdot u^3 \text{ Btu/ft}^2\text{sec} \qquad (6)$$

where $K = 18 \times 10^{-9}$, ρ is the density in slugs/ft^3 , R is the radius in feet, and u is the flight velocity in ft/sec.

The above estimate of the heating rate assumes that the shock is detached. According to Reference 10 the condition for shock detachment on a sphere-capped cone in hypersonic flight is that the coning angle β must be less than about 33 degrees. The heating in the case of sphere-capped cones with higher coning angles, where the shock is attached, is more severe until the coning angle reaches about 60 degrees. For the present study the maximum coning angle was arbitrarily limited at 30 degrees.

Radiation heating has been found to be very small compared to convective heating for all cases of interest here, when computed according to the estimates of References 11 or 12. It can readily be shown that the radiant heating rate at any point in the trajectory,

(say, the point of maximum convective heating rate) varies as $1/R^2$, since $\dot{q}_{rad} \sim \rho^{1.5} R$ (Ref. 12), and $\rho \sim 1/R^2$ at the critical point for a given set of entry conditions. Thus the larger-radius entry body, in spite of the increased shock-layer thickness, experiences lower radiant heating rates. By comparison, the convective heating rate varies as $1/R^{1.5}$. These general conclusions are also supported by the more exact analysis of Reference 14.

B. Entry Trajectory Studies

In order to study the behavior of the Rotornet under conditions of planetary entry, a digital-computer program was written to perform the point-by-point integration of the trajectory equations. The equations of motion assumed a round, non-rotating planet. The temperature of the surface of the Rotornet was computed at each point in the trajectory from the atmospheric density and velocity, using equations (5) and (6). The heating rate at the rim of the coned-back net was taken to be representative of the entire surface.

The Rotornet model used in the trajectory studies was the same as that represented in Figure 4. The model was incorporated into the trajectory program in the form of curve-fit relations which gave drag coefficient and coning deformation as functions of the dynamic pressure and the weight, radius, and spin speed of the disk. Provisions were included for assuming any one of several types of spin-speed control, including constant speed, constant coning angle, constant margin of safety, and constant angular momentum. The details of the trajectory program are discussed in Reference 8.

The computer results for a typical trajectory are shown in Figure 5. It can be seen that the peak coning angle occurs between the points of maximum temperature and maximum deceleration. The spin-speed control for this trajectory provided for a constant margin of safety for the structural fibers; that is, the fiber stress at each point in the trajectory was a fixed fraction of the allowable stress of the material at temperature.

Approximately a hundred trajectories were run, covering a wide variation of mission parameters, Rotornet

size, and material characteristics. It was found that drag modulation (resulting from the coning deformation) had very little effect on the overall trajectory, provided that the maximum coning angle was less than about 35 degrees. It was also found that the classical solutions for entry into an exponential atmosphere with a flat earth[15] could be used, with excellent accuracy, to predict the computer-program results for the peak values of heating rate and deceleration, along with the altitudes and velocities at those points. Figure 6 is a plot of maximum temperature vs. the "loading density" parameter that arises from the classical theory. The computer-trajectory results, plotted on this graph, fell within a scatter band of about $\pm$ 10°F. The value taken for drag coefficient was $C_D = 1.75$.

C. Performance Relations

Since the trajectory results can be predicted using the solutions obtained with the classical exponential-atmosphere theory, it is possible to derive simple algebraic relationships to describe the performance of the Rotornet.

Such relations can be used to compute the weight and size of disk required to perform a given mission, and to shed light on the problem of optimum design. The trajectory relations which are necessary for the derivation (and which are derived in Reference 15) are as follows:

$$u_\tau = u_i e^{-1/6} = .85u_i$$

$$u_N = u_i e^{-1/2} = .61u_i \tag{7}$$

$$\rho_N = 3\rho_\tau$$

Here u is the velocity and ρ the atmospheric density. The subscripts i, τ, and N stand for the initial value and the conditions at the points of maximum temperature and maximum deceleration. Another expression which will be used gives the relation between decelerating force and dynamic pressure:

$$NW = D = \frac{1}{2}\cdot\rho u^2 C_D \pi R^2 \tag{8}$$

The quantity N used here is the load factor (i.e., the deceleration in g's), while W is the total weight of the vehicle.

The desired performance relation can be obtained by expressing the condition for thermal equilibrium in terms of the Rotornet parameters and the initial conditions. Equation (8) may be used to eliminate ρ from the heating equation (6). In addition, the trajectory relations (eq. 7) may be used to express the conditions at the point of maximum heating rate in terms of the initial velocity and the maximum deceleration. For this purpose it is convenient first to establish, from the velocities and densities, the ratio of load factors at the points of maximum heating and maximum deceleration:

$$N_T = \frac{1}{3} \cdot e^{2/3} N_N = .65 N_N \tag{9}$$

On making the various substitutions indicated, it can be seen that the condition for thermal equilibrium at the point of maximum heating is

$$\dot{q}_T^2 = \left[\sigma\epsilon(VF)T_T^4\right]^2 = \frac{1}{3}\cdot 2K^2 u_i^4 \cdot \frac{N_N W}{C_D \pi R^3} \qquad (10)$$

A relation for the Rotornet radius requirement can now be obtained in terms of the allowed temperature and load factor by solving for R in equation (10).

A second performance relation can be developed to give the weight of the Rotornet structure in terms of load, geometry, and size. Since the total force on the coned-back net, from equation (4), is the inertia force of the payload NW_p, the two equations (2) and (4) can be combined to eliminate a_f in order to give the Rotornet radius in terms of the specific strength λ of the structural material and the decelerator weight fraction. Thus:

$$R = \frac{2}{\pi}\cdot\frac{\lambda\cdot\sin\beta}{N}\cdot\frac{W_R}{W_P} \qquad (11)$$

Here $\lambda \equiv s/\rho g$, where the stress s is measured at the hub. Note that the rotor weight fraction is proportional to the radius.

Equation (11), evaluated at $\max \tau$, may now be combined with equation (10) to eliminate R. The resulting expression is the desired performance equation:

$$\left(\frac{W_R}{W_P}\right)^3 = \left(\frac{\pi e}{18}\right)^2 \cdot \frac{K^2}{C_D \cdot \sin^3 \beta_T} \cdot \frac{u_i^4 N_N^4 W}{(\sigma \epsilon V F \tau^4)^2 \cdot \lambda^3} \qquad (12)$$

In the choice of parameters for minimum rotor weight, two critical conditions must be kept in mind: the allowable stress must not be exceeded at the point of maximum temperature, and the critical value of coning angle for maintaining the detached shock must not be exceeded at the point of maximum coning angle. The determination of the more important condition depends on the particulars of the spin-speed control used. In the optimum case, that of operation with constant margin of safety, the designing condition is that the maximum coning angle be limited ($\beta_{max} \leq 30°$), since the decelerator structure is, by definition, equally "safe" at all times. It has been found that, for the materials and mission parameters considered here, this condition is achieved when $\beta_T \leq 25°$. If this value is substituted into

equation (12), the expression can be evaluated for the maximum temperature condition to get

$$\frac{W_R}{W_P} = 6.5 \times 10^{-6} \cdot \frac{u_i^{4/3} N^{4/3} W^{1/3}}{(\sigma T^4)_T^{2/3} \cdot \lambda_T} \tag{13}$$

where the following units must be observed: u , ft/sec; W , lb; σT^4 , Btu/ft^2-sec; λ , ft. The corresponding expression for radius is, from equation (10),

$$R = 2.8 \times 10^{-6} \cdot \frac{u_i^{4/3} N^{1/3} W^{1/3}}{(\sigma T^4)_T^{2/3}} \tag{14}$$

It is shown in Reference 8 that if the optimum condition of constant margin of safety is replaced by the less favorable condition of constant fiber stress, the rotor weight fraction is greater by about 30 percent.

Examination of equation (12) shows that the high-temperature characteristics of the structural material affect the rotor weight fraction only through the term $[\sigma \epsilon (VF) T^4]^{2/3} \cdot \lambda$. The lowest weight fraction for a given material is obtained by choosing the maximum temperature

τ_T so as to coincide with the maximum value of this parameter. This parameter also forms a basis for comparing different materials. Figure 7 shown the strength-vs.-temperature characteristics of various structural-fiber materials. The importance of high-temperature capability for candidate materials for the Rotornet is shown by Figure 8, which is based on Figure 7.

Figures 9 and 10 are plots of the performance equations (13) and (14). The structural material was taken to be silica fiber with a safety factor of 5. It can be seen that the structural-weight fraction for the Rotornet is of the order of a few percent for payloads of typical size, even for escape velocity. The curve of rotor thickness represents the thinnest portion of the disk, assuming the disk to be constructed of circular-cross-section fibers with square packing.

The performance relations show that the weight of the spinning-disk decelerator is least for missions with low values of maximum deceleration. This property arises from the nature of the heat-rejection mechanism;

since the critical factor is the maximum heating rate, rather than the total quantity of heat rejected, the heating problem becomes less severe, for a given initial velocity, if the heating time (as well as the deceleration time) can be prolonged. By contrast, ablator weights show a slight increase with an increase in the length of the heat pulse.

Performance relations can also be derived for the case of lifting flight with a fixed L/D and for the case of equilibrium glide at superorbital velocity. The latter case is particularly interesting, in that it indicates that a decelerator capable of reentering the earth's atmosphere with hyperbolic velocity can be made with a structural weight which is only a few percent of the payload weight. The L/D assumed for this calculation was 0.2, which is, in principle, well within the capability of a spinning disk in hypersonic flow.

V. FLIGHT DYNAMICS

Dynamic analysis of the Rotornet in axial flight has revealed the existence of three distinct modes of dynamic instability. The first is a violent divergence that occurs at high coning angles when the center of gravity is located too far aft of the hub plane.[8] The instability results from the fact that the static compressive load in the structure connecting the payload to the hub plane creates a destabilizing moment similar to that in a compressively loaded column. For high axial deceleration and correspondingly large coning angles, the stiffening effect of the gyroscopic forces acting on the rotor disk is insufficient to overcome the destabilizing moment and the rotor topples. A stability boundary for "strong column instability", is shown in Figure 11 for a typical configuration. The effect may be alleviated by increasing the hub radius and may be eliminated entirely by placing the center of gravity forward of the hub plane. When aerodynamic damping effects are added to the stability analysis, it is found that the region of strong column

instability is bordered by a region of mild instability, in which the amplitude increases at a rate that is generally less than one percent per revolution.

The second type of dynamic instability is a spiral divergence that is common to all helicopter-like devices.[8,20] In this mode the vehicle executes a slowly diverging helical motion accompanied by a slight tilt of the vehicle away from the axis of the helix. Relative motion between the rotor disk and the hub plane is small. The instability disappears for sufficiently large coning angles and is insensitive to center of gravity position and hub radius.

As shown in Figure 11, spiral instability and column instability are avoided by a vehicle with a forward center of gravity operating with a coning angle greater than about 13 degrees. Smaller coning angles can be avoided except possibly during the initial portion of the planetary entry trajectory. Spiral instability is not expected to be a serious problem because the rate of divergence is very small (less than one percent per revolution) and because the elapsed time between effective

contact with the sensible atmosphere and the development of a sufficiently large coning angle is short (See Figure 5). It is also possible to eliminate spiral instability at low coning angles by means of an active autopilot that tilts the rotor hub relative to the axis of the vehicle in response to error signals from an attitude reference.[8]

The third type of dynamic instability that has been identified during investigation of the Rotornet is a travelling wave flutter in which waves travel around the rotor disk at a fraction of the rotational speed. From two to six waves with impressively large amplitudes have been observed by spinning flexible disks in still air and during tests in a low-speed wind tunnel,[21] Figure 12 is a photograph of a Rotornet with rim impellers in tethered autorotating flight taken just prior to collapse. The figure illustrates both spiral instability and two-wave travelling wave flutter. An example of stable flight is shown in Figure 13.

Analysis of the travelling wave flutter phenomenon in subsonic flight reveals that the critical parameter

governing its occurrence is the ratio of the apparent mass of the fluid to the mass of the rotor disk. In addition to a small amount of damping, either structural or aerodynamic, is required to prevent flutter. Figure 14 shows a subsonic stability boundary for a Rotornet with aerodynamic impeller tabs distributed around the rim. The mass parameter, μ, is the ratio of the mass of a sphere of air with the same diameter as the rotor disk, to the mass of the rotor disk. The damping parameter, B, is the ratio of tip speed to axial descent speed multiplied by the ratio of impeller area to total disk area. It is seen that stable flight cannot be achieved for $\mu > 3$, or for $B < .05$. The critical flutter mode has two waves.

The restriction to small values of the mass parameter is a severe limitation for low altitude subsonic flight in the earth's atmosphere and may effectively eliminate the Rotornet as a terminal descent device for landing on earth. The situation with regard to a Mars landing is much more favorable due to the lower atmospheric density. Values of μ for tentative designs of Martian entry vehicles are generally around 1.0 .

An analysis has also been made[21] of travelling wave flutter in hypersonic flight. In this regime apparent mass is not a consideration and the critical parameter is the aerodynamic damping provided by rim impellers. Flutter boundaries for hypersonic travelling wave flutter are shown in Figure 15. It is seen that the number of waves in the flutter mode will be large and that the surface area of the impeller tabs should at least be equal to 14% of total disk area. The coning angle is significant only for flutter with a small number of waves.

Rim impellers designed as aerodynamic damping devices should be torsionally unconstrained at their connections to the rim, and should be mass balanced to a point forward of the aerodynamic center. Centrifugal force provides a spring rate that resists pitching motions of the impellers.

Rim impellers are also required to maintain rotor speed in the presence of aerodynamic friction torque particularly in the terminal flight phase. Calculations show that, with impellers of sufficient size to prevent

travelling wave flutter, the lift coefficient required for autorotating subsonic flight is easily achieved.

It can also be shown[8] that aerodynamic drive is not necessary in the hypersonic portion of the entry trajectory provided that the Rotornet is pre-spun by rocket motors prior to entry. Speed decay due to aerodynamic friction is not significant until well after peak deceleration.

An interesting possibility is the use of chordwise mass balance of the rim impellers to produce speed stability without the aid of an active control system. It is not difficult to calculate the balance required to maintain a given rotor speed for each flight regime. Achieving a satisfactory compromise of the various requirements may be more difficult.

Rotary winged vehicles are capable of trimmed lifting flight provided that some parameter of the system is varied cyclicly with azimuth position. In the case of the Rotornet a convenient parameter to vary is the tilt of the hub plane relative to the axis of the vehicle. The lift to drag ratio that can be achieved by such a system

may be estimated from the following formula

$$L/D = \frac{3}{2} \cdot \frac{y_{ac}}{R \cdot \sin\beta} \tag{15}$$

where R is the rotor radius, β is the coning angle and y_{ac} is the lateral offset of the center of gravity of the vehicle relative to an axis that is perpendicular to the hub plane. It will be noted that large L/D ratios can be achieved when the coning angle is small, i.e., when the drag is small, so that the primary limitation is on lift rather than on the L/D ratio.

The cyclic control system will require a mechanical swash-plate between the hub and the fuselage of the vehicle and some means (probably small aerodynamic surfaces) to balance the torque on the fuselage due to bearing friction. Rotational isolation of the fuselage from the rotor will be required for a man-rated vehicle in any case. For such systems the addition of a swash plate to provide lateral control and trimmed lifting flight is not a serious complication.

For unmanned vehicles it is permissible for the fuselage to rotate. Thus, if there is no requirement for lift, and if rotor speed can be adequately controlled by the mass balance of rim impellers, unmanned Rotornet entry vehicles can be built without bearings, swash plates or active control systems of any kind.

VI. CONCLUSIONS AND RECOMMENDATIONS

On the basis of the feasibility study which is described here, it appears that the spinning disk is potentially an attractive hypersonic decelerator for planetary entry. It can be shown that extremely low decelerator weight fractions are possible with this concept for a wide range of mission parameters, at a cost of some increase in mechanical complexity over the conventional systems. The concept seems especially promising for two types of missions: those for which the entry deceleration must be accomplished in low-density atmosphere, and those which require low levels of deceleration with high initial velocities.

This approach represents a sharp departure from existing decelerator technology. There are, therefore, a number of technical areas in which experience must be gained before the full potential of the concept can be known or realized. The areas of greatest immediate interest are those having to do with the aerothermodynamics of the spinning cone in hypersonic flow, such as the prediction

of friction torque, the effects of porosity, heating distribution in non-axial flight, and the design of rim vanes for driving torque and flutter suppression.

The application for which the Rotornet appears to offer the greatest potential advantage is that of manned reentry at superorbital velocities. In addition to the low weight fraction, the large spinning disk promises to provide the capability for high-altitude, hypersonic gliding and maneuvering. While it is doubtful that a given disk could be used for more than one entry mission, the cost of replacing a disk should be small compared to the cost of refurbishing a conventional ablation-protected gliding vehicle. In this respect the Rotornet is similar to the parachute; eventually the logistics could be similar. For operations which require a large amount of reentry traffic (such as a "shuttle service" to and from an orbiting station), the Rotornet system could provide a very attractive combination of low airframe weight, good maneuvering capability, and low refurbishing cost.

Another type of mission in which the low-loading decelerator offers many advantages is in the exploration of planetary atmospheres. A very light vehicle can decelerate at higher altitude and descend more slowly, thereby allowing more time and better conditions for taking and transmitting data. A Rotornet for a Mars Probe-Lander, for example, could be a one-piece design, provided the payload is permitted to spin. If a shallow entry could be enforced, the Rotornet would offer a large saving in the weight of the entry decelerator; for 90-degree entry the Rotornet weight is competitive with proposed ablative devices. Furthermore, the Rotornet would be suitable for terminal descent, thereby eliminating the parachute and its associated ejection and deployment systems. Thus, for this application, the Rotornet promises to be both lighter and less complicated than conventional deceleration systems, in addition to offering the advantages of the low-loading decelerator.

In summary, it may be concluded that the concept of the spinning-disk decelerator should be pursued. It is generally recognized that the radiation-cooled low-loading

decelerator offers many operational advantages over the hotter, more dense systems. The technique of spinning the surface to hold it erect promises to make the radiation-cooled decelerator a practical matter, by permitting very large surface areas at attractive values of total decelerator weight.

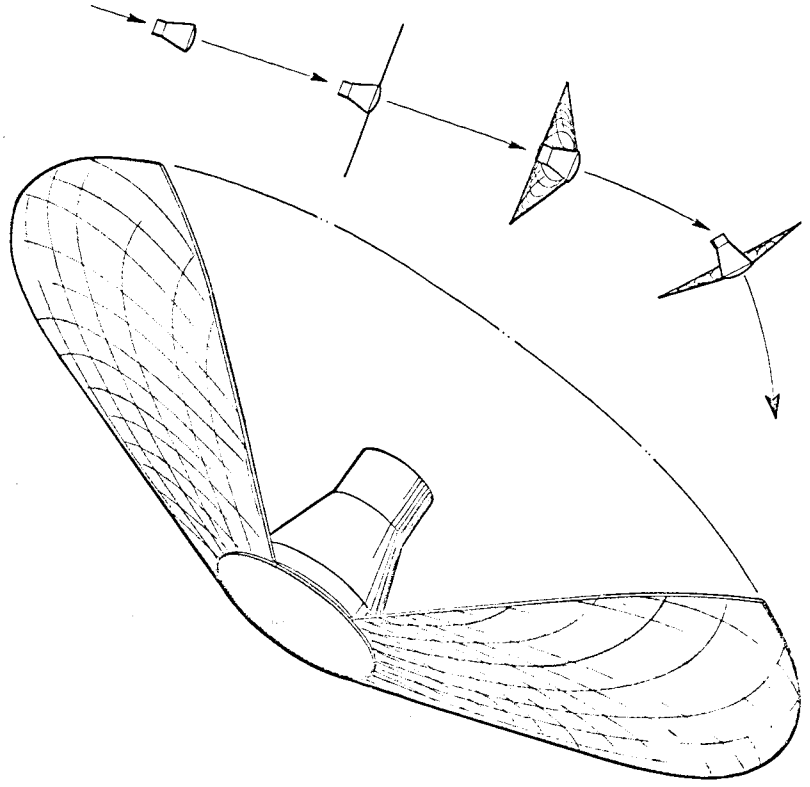

Figure 1 — Spinning-Disk ("Rotornet") Decelerator

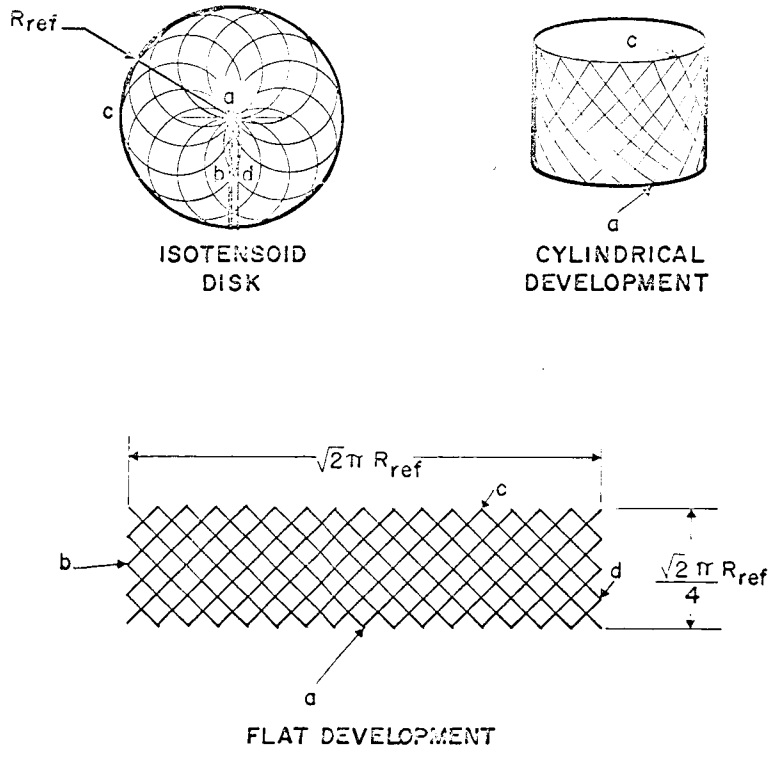

Figure 2 — Isotensoid Disk: Fiber Pattern and Development

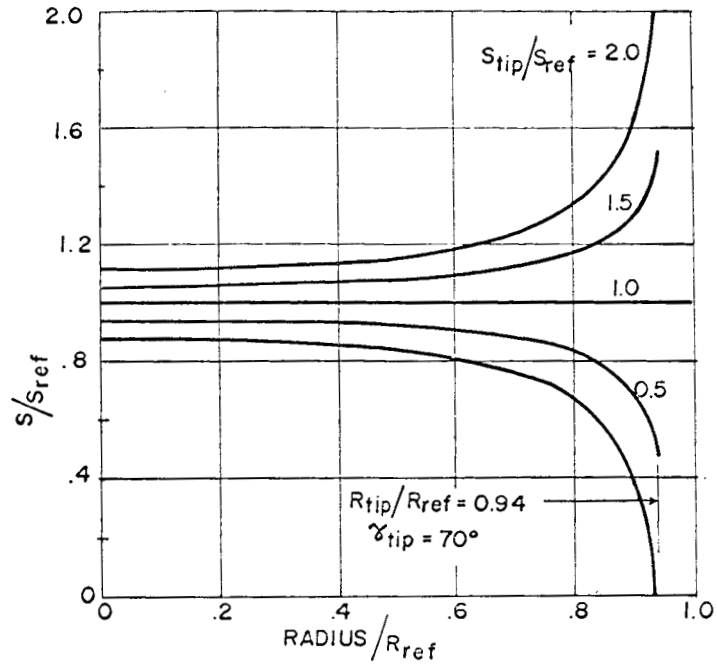

Figure 3 — Stress Distribution In Truncated Disk With Various Sizes of Tip Weights

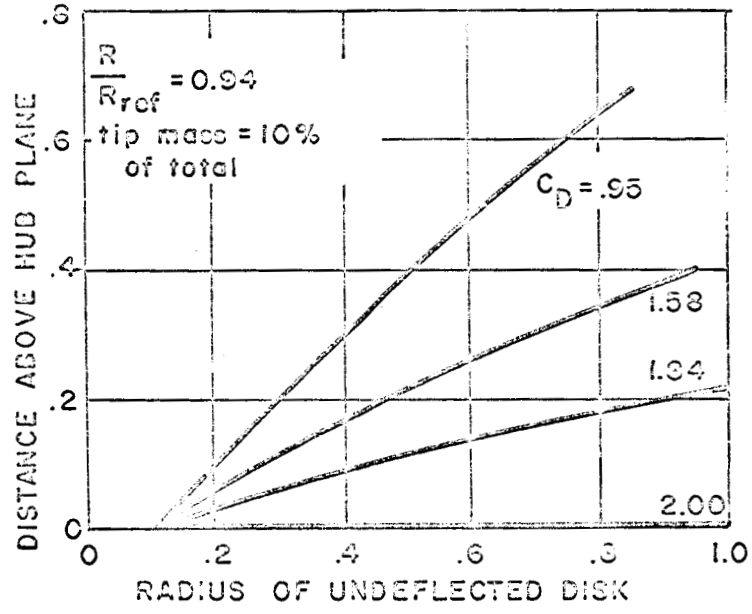

Figure 4 — Meridional Curves and Drag Coefficients For Coned-Back Rotornet

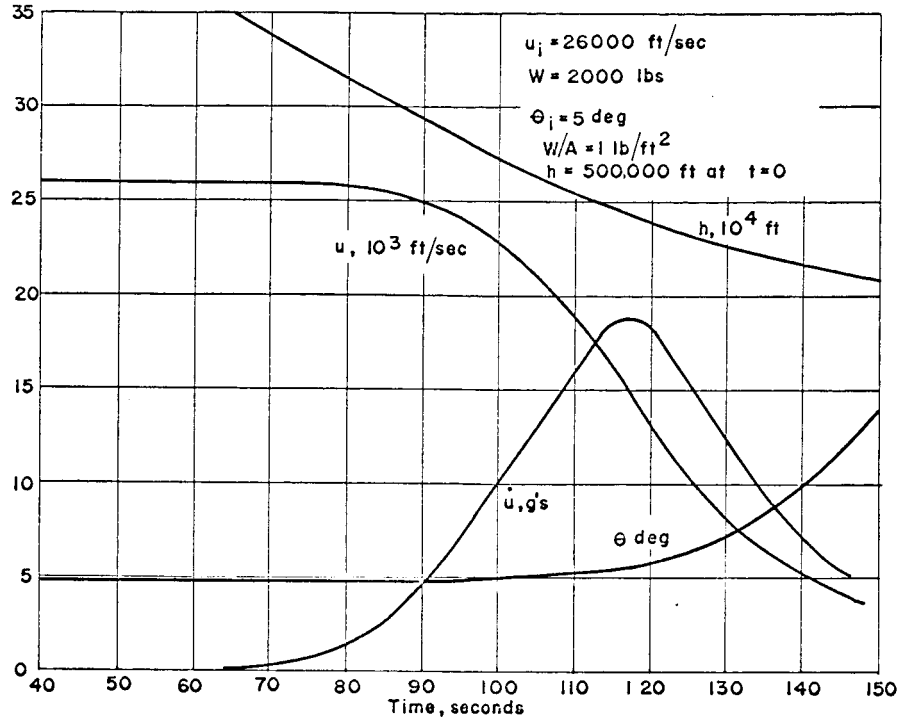

a. Vehicle Motion

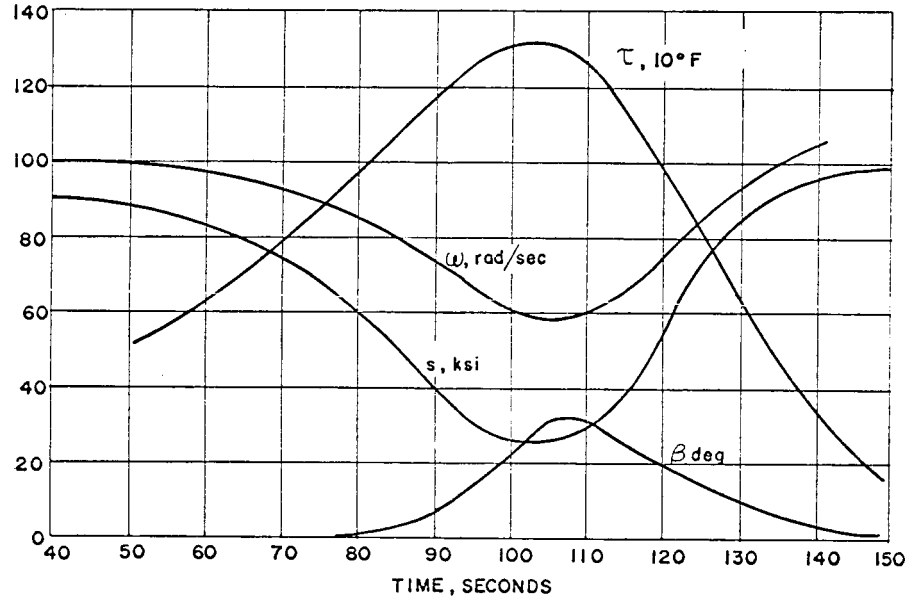

b. Rotornet Response

Figure 5 — Typical Ballistic Trajectory For Earth Entry With Constant Margin of Safety (X-37B Glass Fiber)

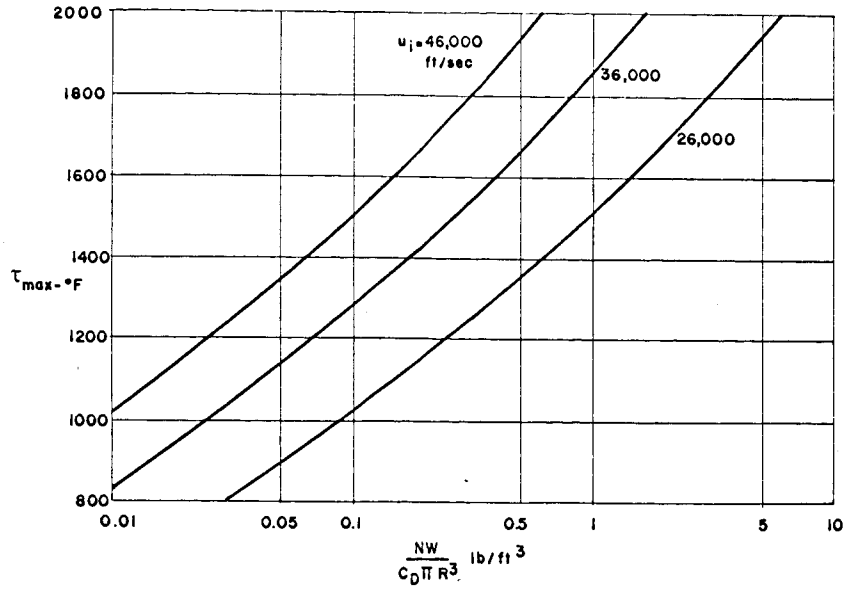

Figure 6 —— Maximum Temperature Vs. Loading-Density Parameter

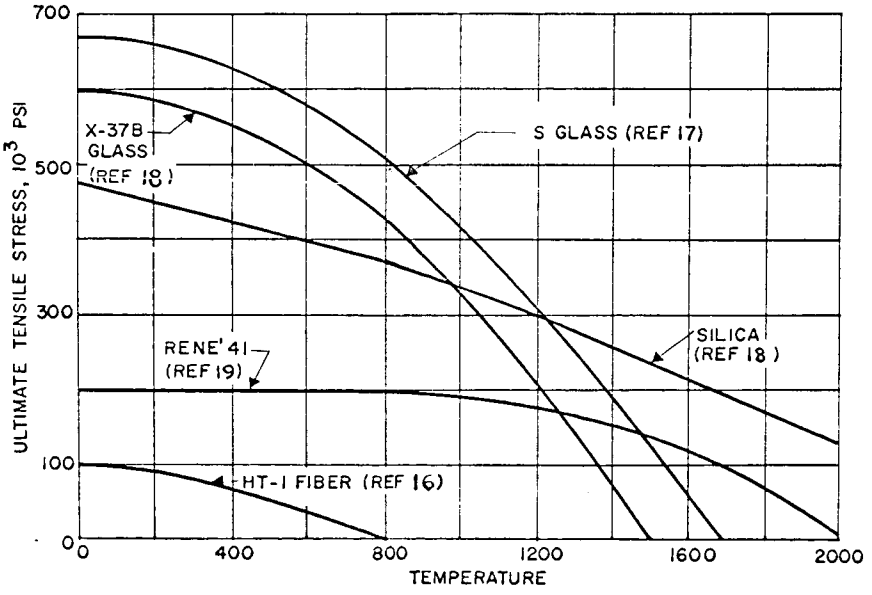

Figure 7 —— Strength vs. Temperature For Various Structural Fibers

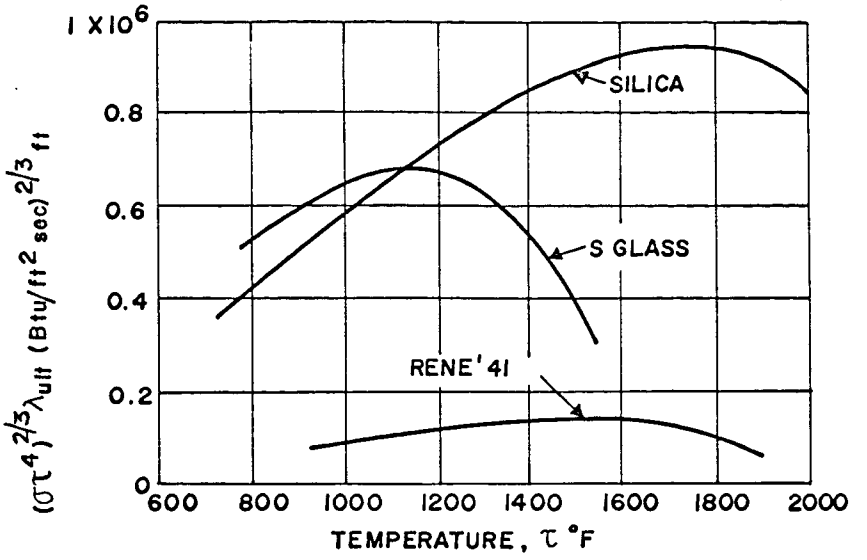

Figure 8 —— Temperature-Weight Parameter For Performance Relations

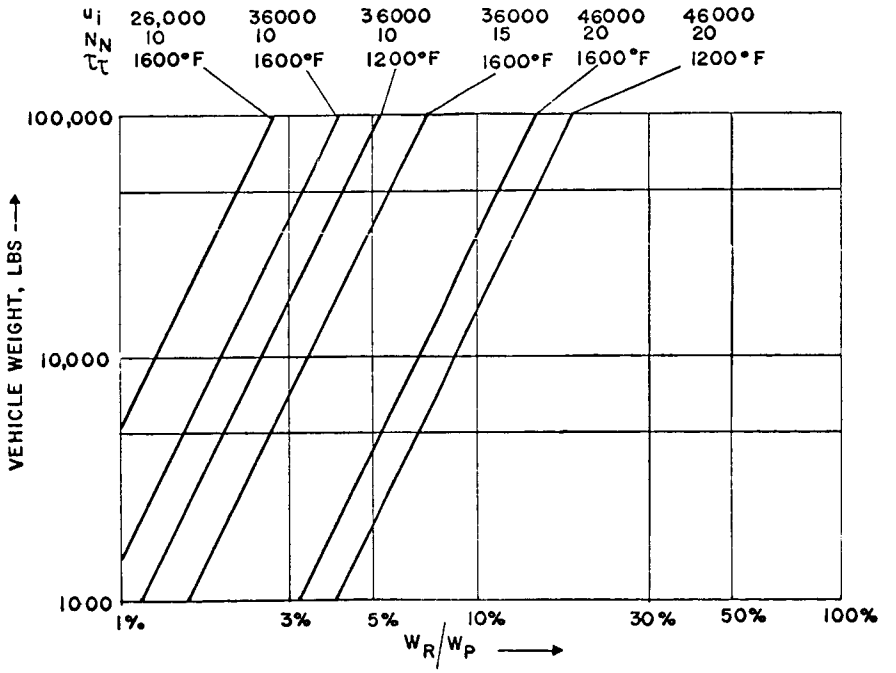

Figure 9 —— Rotornet Weight Fraction For Ballistic Entry (Silica Fiber With Safety Factor of 5)

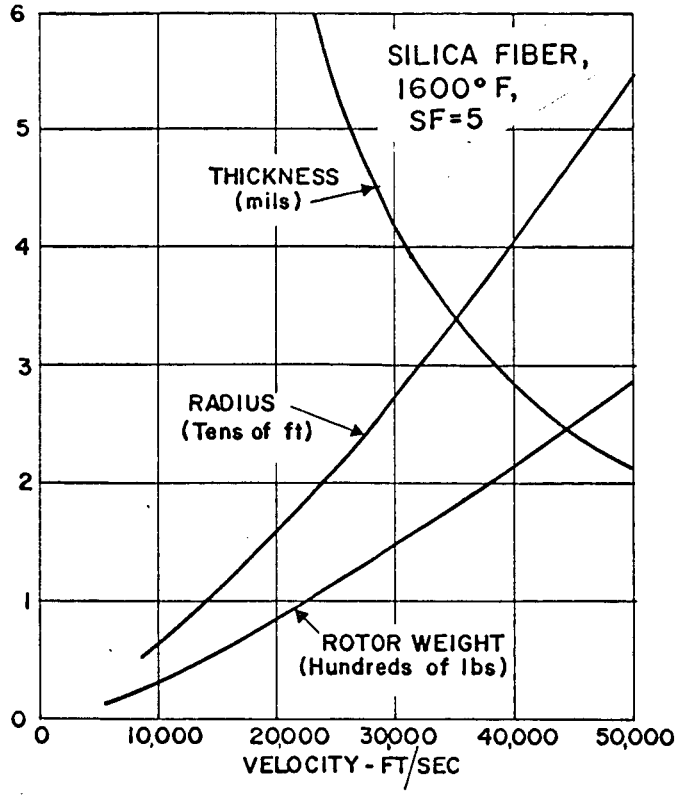

Figure 10 — Rotornet Size vs. Initial Velocity For 10,000-lb Vehicle (10 g's, 1600°F, Silica, SF = 5)

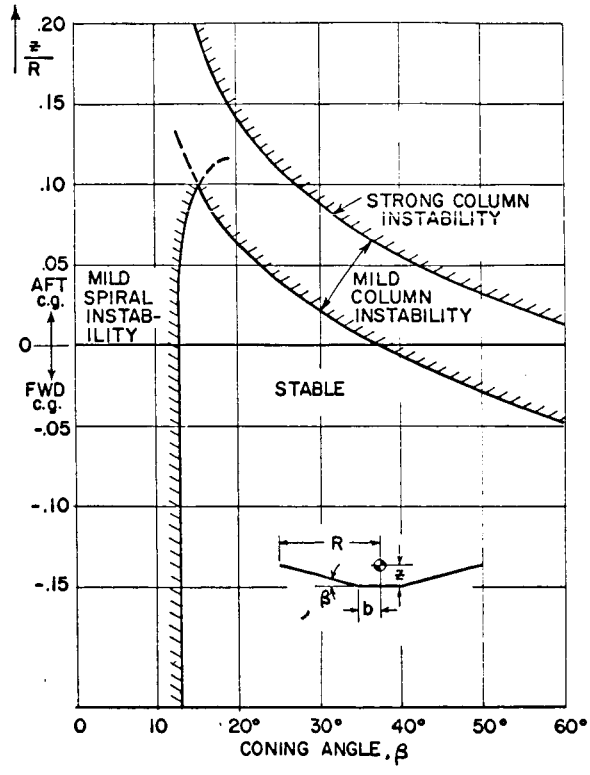

Figure 11 — Column and Spiral Stability Boundaries, b/R = 0.1

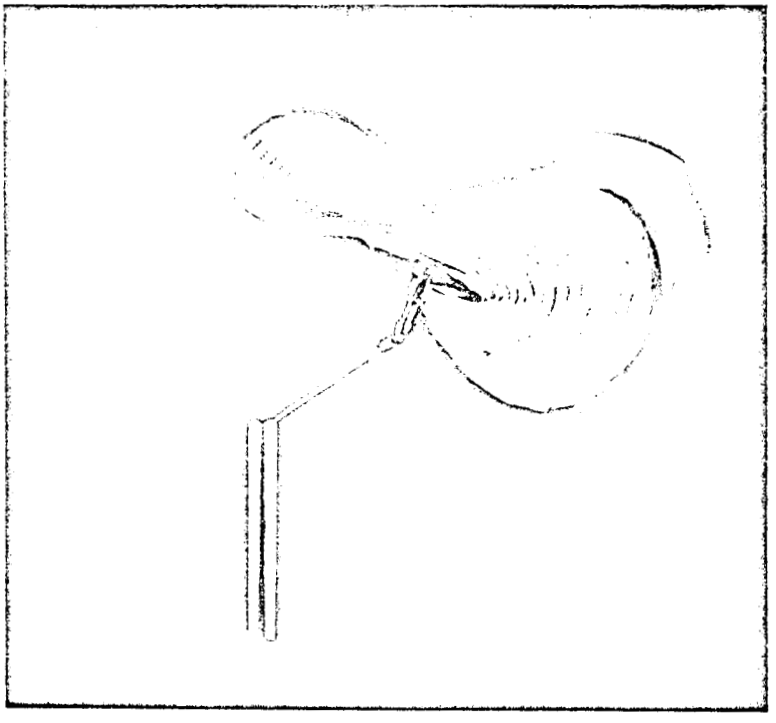

Figure 12 —— Unstable Rotornet In Tethered Flight

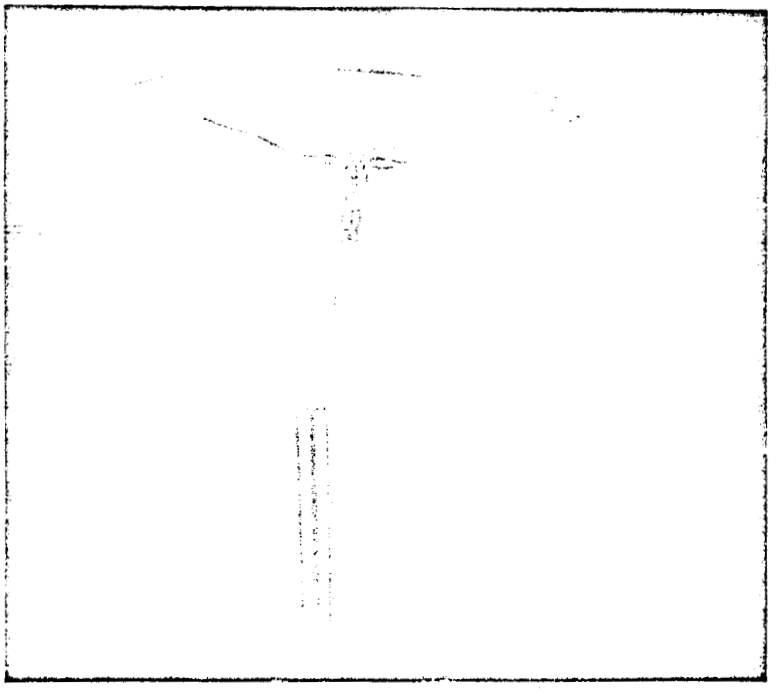

Figure 13 —— Stable Rotornet In Tethered Flight

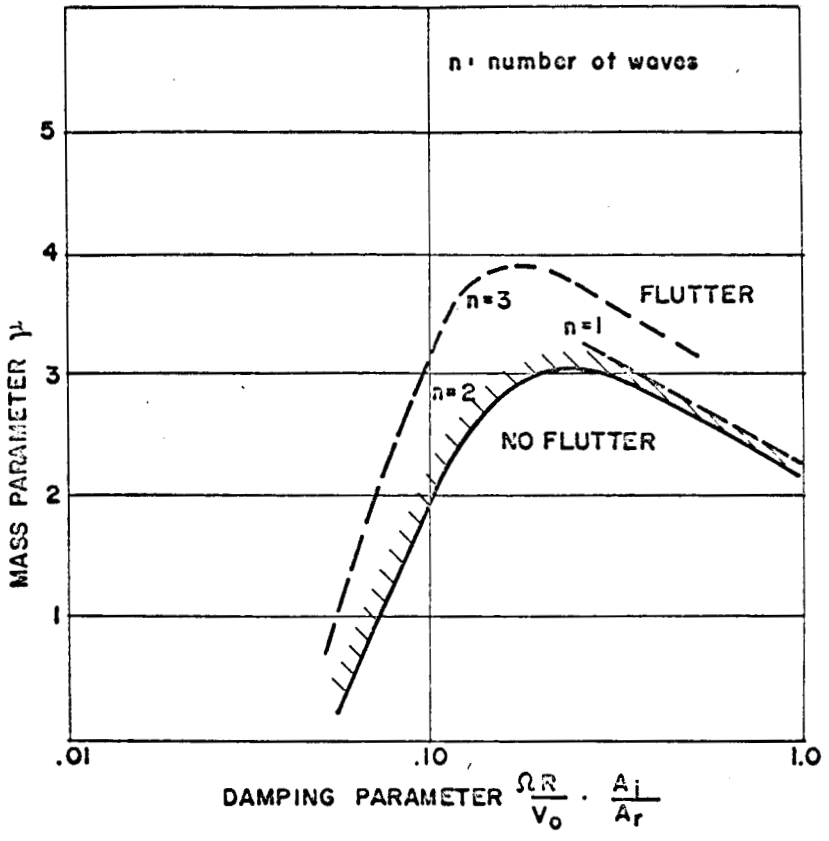

Figure 14 — Subsonic Travelling-Wave Flutter Boundary

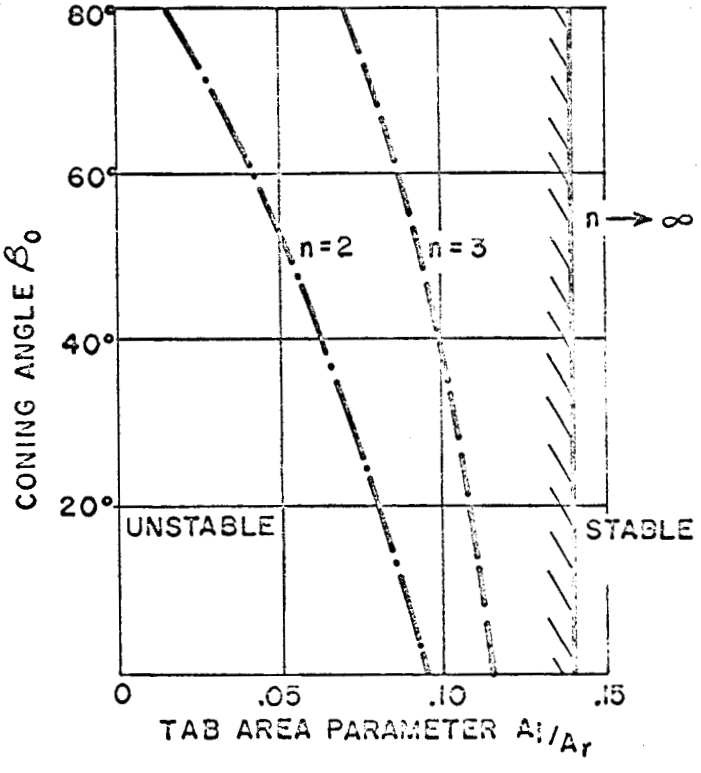

Figure 15 — Hypersonic Travelling-Wave Flutter Boundaries

REFERENCES

1. Eggers, Alfred J., Jr.: "The Possibility of a Safe Landing." Space Technology, Part II, Chapter 13. John Wiley & Sons, Inc., 1959.

2. Gazley, Carl, Jr.: "Atmospheric Entry." Handbook of Astronautical Engineering, Chapter 10. McGraw-Hill Book Company, 1961.

3. "Performance of End Design Criteria For Deployable Aerodynamic Decelerators." ASD-TR-61-579, December 1963.

4. "Study of A Drag Brake Satellite Recovery System." ASD TR-61-348, January 1962.

5. Roberts, Leonard: "Entry Into Planetary Atmospheres." Astronautics and Aeronautics. October 1964, pp. 22-29.

6. Anderson, Roger A.: "Space Technology - 1964." Astronautics and Aeronautics. December 1964, pp. 14-20.

7. Kyser, A. C.: "The Uniform Stress Spinning Filamentary Disk." NASA CR-106, May 29, 1964.

8. Kyser, A. C.: "The Rotornet: A High-Performance Hypersonic Decelerator For Planetary Entry." NASA CR-247, June 1965.

9. MacNeal, Richard H.: Mechanics of a Coned Rotating Net." NASA CR-248, July 1965.

10. Lees, Lester: "Laminar Heat Transfer of Blunt-Nosed Bodies At Hypersonic Flight Speeds." Jet Propulsion. April 1956.

11. Lees, Lester: "Recovery Dynamics-Heat Transfer At Hypersonic Speeds In A Planetary Atmosphere." Space Technology, Part II, Chapter 12. John Wiley & Sons, Inc., 1959.

12. Hildebrand, R. B.: "Aerodynamic Fundamentals." Handbook of Astronautical Engineering, Chapter 5. McGraw-Hill Book Company, 1961.

13. Stainback, P. Calvin: Pressure And Heat Transfer Measurements On The Flat Face of Blunted 10° Half-Cone Body (Semidisk) At A Mach Number of 6.15 . NASA TN D-1628, May 1963.

14. Page, William A.; and Arnold, James O.: "Shock-Layer Radiation of Blunt Bodies At Reentry Velocities." NASA TR R-193, April 1964.

15. Allen, H. Julian; and Eggers, A. J., Jr.: "A Study of The Motion And Aerodynamic Heating of Ballistic Missiles Entering The Earth's Atmosphere At High Supersonic Speeds." NACA TR 1381, 1958.

16. Chu, Chauncey C.; Gardella, Joseph W.; and Kaswell, Ernest R.: "Research Leading To Optimum Fibrous Structures of HT-1 Yarn." ML TDR 64-78, January 1964.

17. "A Comparative Properties Analysis." Owens-Corning Fiberglas Corporation, NY-AD-64-3A, New York, N.Y., September 1964.

18. Otto, W. H.: "Properties of Glass Fibers At Elevated Temperatures." DDC AD 228 851, August 1959.

19. Johnson, Dennis E.; Newton, Emerson H.; et al.: "Metal Filaments For High Temperature Fabrics." ASD TR 62-180, February 1962.

20. Schuerch, H. U.; and MacNeal, R. H.: "Deployable Centrifugally Stabilized Structures For Atmospheric Entry From Space." NASA CR-69, July 1964.

21. MacNeal, R. H.: "Travelling Wave Flutter of Rotating Disks." Astro Research Corporation Report ARC-R-195, September 1965.